

Effect of Couette Flow on Electroconvective Vortices

Yifei Guan and Igor Novosselov [§]

Department of Mechanical Engineering, University of Washington, Seattle, U.S.A. 98195

Institute for Nano-Engineered Systems, University of Washington, Seattle, U.S.A. 98195

Abstract—Numerical simulation of Electroconvective vortices behavior in the presence of Couette flow between two infinitely long electrodes is investigated. The two-relaxation-time Lattice Boltzmann Method with fast Poisson solver solves for the spatiotemporal distribution of flow field, electric field, and charge density. Couette cross-flow is applied to the solutions after the electroconvective vortices are established. Increasing cross-flow velocity deforms the vortices and eventually suppresses them when threshold values of shear stress are reached.

Keywords: Lattice Boltzmann Method, Fast Poisson Solver, electroconvection stability, Couette flow

I. INTRODUCTION

Insights into multiphysics interactions are crucial for understanding Electrohydrodynamics (EHD flows: (1) the electric field from the potential difference between the anode and cathode and its modifications by the space charge effects; (2) the ion motion in the electric field; (3) the interaction between the motion of ions and the neutral molecules; and (4) the inertial and viscous forces in the complex flow. As a subset of EHD, electroconvection (EC) is a phenomenon where convective transport is induced by unipolar discharge into a dielectric fluid [1-20]. The EC stability problem was first analyzed by a simplified non-linear hydraulic model [21, 22] and linear stability analysis without charge diffusion [23, 24]. Atten & Moreau [25] showed that in the weak-injection limit, $C \ll 1$, where C is the charge injection level, the flow stability is determined by the criterion $T_c C^2$, where T_c is the linear stability threshold for the electric Rayleigh number T — a ratio between electric force to the viscous force. In the space-charge-limited (SCL) injection, $C \rightarrow \infty$, the flow stability is determined by T_c only. The experimental observations [26, 27] have shown that, for the SCL scenario, $T_c = 100$, while linear stability analysis suggests $T_c = 160.45$ for the same conditions [25]. It was suggested that the discrepancy is due to the omission of the charge diffusion term in the analysis [28]. The effect of charge diffusion was investigated using linear stability analysis with a Poiseuille flow [11] and by non-linear analysis using a multiscale method [16]. It was shown that the charge diffusion has a non-negligible effect on T_c and the transient behavior depends on the Reynolds number (Re) [11, 16].

To gain insight into the complexity of the EC flow, the problem can be investigated by numerical simulations. The earlier finite difference model simulations have shown that strong numerical diffusivity may contaminate the model [2]. Other numerical approaches include the particle-in-cell method [29], finite volume method with the flux-corrected transport scheme [30], total variation diminishing scheme [4, 7, 13-15], and the method of characteristics [3]. Lattice Boltzmann model (LBM) was shown to predict the linear and finite amplitude stability criteria of the subcritical bifurcation in the EC flow [17-20] for both 2D and 3D flow scenarios. This unified LBM transforms the elliptic Poisson equation into a parabolic reaction-diffusion equation and introduces artificial coefficients to control the evolution of the electric potential.

The EC stability problem is analogous to Rayleigh-Benard convection (RBC) [20, 31-36]. Of particular interest is the suppression of the RBC cells in the cross-flow [37]. A non-dimensional group Gr / Re^2 , the ratio of buoyancy to the inertia force, was used to parametrize the effect of the applied shear, where Gr is the Grashof number. For $Gr / Re^2 > 10$, the effect of the cross-flow is insignificant, while for $Gr / Re^2 < 0.1$, the effect of the buoyancy can be neglected. In the EC flow scenario, 2D finite volume simulations of Poiseuille flow show that the critical electric Rayleigh number, T_c , depends on the Re and ion mobility parameter, M [12].

In this paper, we investigate the EC stability in the cross-flow between two parallel electrodes. The segregated solver used in the study combined a two-relaxation-time LBM modeling fluid and charged species transport and a Fast Fourier Transform Poisson solver to solve for the electric field directly [38]. Couette cross-flow scenario provides shear

[§] ivn@uw.edu

stress. A subcritical bifurcation is described by the ratio of the electrical force to the viscous force.

II. METHODOLOGY

The governing equations for EHD flow include the Navier-Stokes equations (NSE) with the electric forcing term $\mathbf{F}_e = -\rho_c \nabla \varphi$ in the momentum equation, the charge transport equation, and the Poisson equation for electric potential.

$$\nabla \cdot \mathbf{u} = 0, \quad (1)$$

$$\rho \frac{D\mathbf{u}}{Dt} = -\nabla P + \mu \nabla^2 \mathbf{u} - \rho_c \nabla \varphi, \quad (2)$$

$$\frac{\partial \rho_c}{\partial t} + \nabla \cdot [(\mathbf{u} - \mu_b \nabla \varphi) \rho_c - D_c \nabla \rho_c] = 0, \quad (3)$$

$$\nabla^2 \varphi = -\frac{\rho_c}{\varepsilon}, \quad (4)$$

where ρ is the density, μ is the dynamic viscosity, $\mathbf{u} = (u_x, u_y)$ is the velocity vector field, P is the static pressure, μ_b is the ion mobility, D_c is the ion diffusivity, ρ_c is the charge density, ε is the electric permittivity, and φ is the electric potential. The electric force provides a source term in the momentum equation (Eq. 2) [11, 39-41]. Non-dimensional analysis of the governing equations NSE (Eq. 1-4) yields:

$$\nabla^* \cdot \mathbf{u}^* = 0 \quad (5)$$

$$\frac{D^* \mathbf{u}^*}{D^* t^*} = -\nabla^* P^* + \frac{M^2}{T} \nabla^{*2} \mathbf{u}^* - CM^2 \rho_c^* \nabla^* \varphi^*, \quad (6)$$

$$\frac{\partial^* \rho_c^*}{\partial^* t^*} + \nabla^* \cdot \left[(\mathbf{u}^* - \nabla^* \varphi^*) \rho_c^* - \frac{1}{Fe} \nabla^* \rho_c^* \right] = 0. \quad (7)$$

$$\nabla^{*2} \varphi^* = -C \rho_c^*, \quad (8)$$

where the asterisk denotes the non-dimensional variables. In the absence of cross-flow, non-dimensional governing equations yield four dimensionless parameters describing the system's state [4, 6, 7, 9, 11-20].

$$M = \frac{(\varepsilon / \rho)^{1/2}}{\mu_b}, \quad T = \frac{\varepsilon \Delta \varphi_0}{\mu \mu_b}, \quad C = \frac{\rho_0 H^2}{\varepsilon \Delta \varphi_0}, \quad Fe = \frac{\mu_b \Delta \varphi_0}{D_c}, \quad (9)$$

where H is the distance between the electrodes (two infinite plates), ρ_0 is the injected charge density at the anode, and $\Delta \varphi_0$ is the voltage difference between the electrodes. The physical interpretations of these parameters are as follows: M is the ratio between hydrodynamic mobility and the ionic mobility; T is the ratio between electric force to the viscous force; C is the charge injection level [11,

16]; and Fe is the reciprocal of the charge diffusivity coefficient [11, 16].

III. RESULTS

To model EC vortices, the hydrostatic base-state is perturbed using wave-form functions with a small amplitude that satisfies the boundary conditions and continuity equation:

$$\begin{aligned} u_x &= L_x \sin(2\pi y / L_y) \sin(2\pi x / L_x) \times 10^{-3} \\ u_y &= L_y \left[\cos(2\pi y / L_y) - 1 \right] \cos(2\pi x / L_x) \times 10^{-3} \end{aligned} \quad (10)$$

The physical domain size $L_x = 1.22m$ and $L_y = 1m$ limits the perturbation wavenumber to $\lambda_x = 2\pi / L_x \approx 5.15(1/m)$, yielding the most unstable mode under the conditions $C = 10, M = 10$ and $Fe = 4000$ [18]. The electric Nusselt number, $Ne = I / I_0$, serves as a flow stability criteria, where

I is the cathode current for a given solution and I_0 is the cathode current for the hydrostatic solution [4, 18]. For cases where EC vortices exist, $Ne > 1$. For a strong ion injection, the EC stability largely depends on T , so, in this analysis, T is varied, while other non-dimensional parameters are held constant at $C = 10, M = 10$, and $Fe = 4000$ [42].

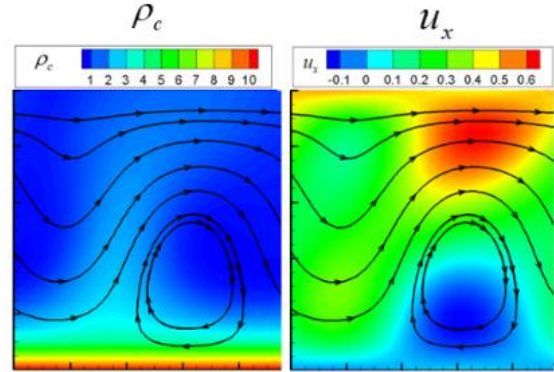


FIG. 1. Charge density and x-direction velocity contour of the EC with cross-flow. Couette flow with $u_{wall} = 0.5m/s$; one of the two vortices is suppressed.

The Couette cross-flow is added after EC vortices are established by assigning constant velocity of the upper wall. FIG. 1 shows the charge density and x-direction velocity for Couette cross-flow ($u_{wall} = 0.5m/s$). The Couette cross-flow stretches the vortices in the direction of the bulk flow and may eliminate one of the two vortices. The vortex suppression is due to the interaction of the vortex's x-velocity components with cross-flow; these interactions are the strongest near the walls where x-velocity are the greatest. For example, the clockwise vortex will be deformed at some oblique angle as in x-direction (streamwise) flow accelerates

the upper region of the vortex and slows down the bottom region (relative to the mean velocity). This is reversed in the case of the counterclockwise rotating vortex. For strong cross-flow, both vortices are eliminated, and $I=I_0$, $Ne=1$. Here, the EC contribution to the flow field is negligible at higher values of shear stress (higher velocity), and the flow field is the same as the applied cross-flow.

FIG. 2 shows the extended stability analysis of EC with and without cross-flow [38] by introducing a finite velocity of the upper wall (cathode). For a constant T , Ne decreases as U_{wall} increases. The applied shear stress reduces the EC effect on the flow.

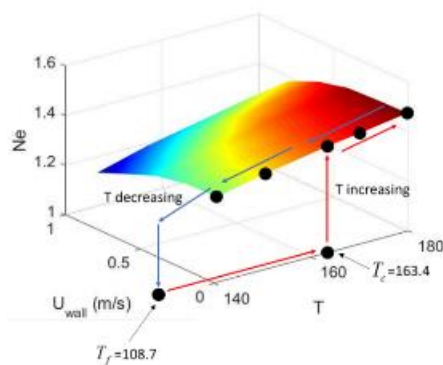


FIG. 2. Electric Nusselt number depends on the electric Rayleigh number T and applied velocity of the upper wall U_{wall} for Couette type cross-flow.

IV. CONCLUSION

The 2D numerical study extends the EC stability analysis to Couette flow between two infinitely long parallel electrodes. The numerical approach utilizes the two-relaxation-time LBM to solve the flow and charge transport equations and a Fast Poisson Solver to solve the Poisson equation. Shear stress from the applied cross-flow deforms the EC vortices due to the interaction of streamwise velocity components resulting in vortex suppression at high crossflow velocities.

ACKNOWLEDGMENT

This research was supported by the DHS Science and UK Home Office; grant no. HSHQDC-15-531 C-B0033, by the National Institutes of Health, grant NIBIB U01 EB021923 and NIBIB R42ES026532 subcontract to UW

REFERENCES

[1] B. Malraison and P. Atten, Chaotic behavior of instability due to unipolar ion injection in a dielectric liquid, *Physical Review Letters* **49**, 723 (1982).
 [2] A. Castellanos and P. Atten, Numerical modeling of finite amplitude convection of liquids subjected to unipolar injection, *IEEE transactions on industry applications*, 825 (1987).
 [3] K. Adamiak and P. Atten, Simulation of corona discharge in point-plane configuration, *Journal of electrostatics* **61**, 85 (2004).

[4] P. Traoré and A. Pérez, Two-dimensional numerical analysis of electroconvection in a dielectric liquid subjected to strong unipolar injection, *Physics of Fluids* **24**, 037102 (2012).
 [5] R. Kwak, V. S. Pham, K. M. Lim, and J. Han, Shear flow of an electrically charged fluid by ion concentration polarization: scaling laws for electroconvective vortices, *Physical review letters* **110**, 114501 (2013).
 [6] P. Traoré and J. Wu, On the limitation of imposed velocity field strategy for Coulomb-driven electroconvection flow simulations, *Journal of Fluid Mechanics* **727** (2013).
 [7] J. Wu, P. Traoré, P. A. Vázquez, and A. T. Pérez, Onset of convection in a finite two-dimensional container due to unipolar injection of ions, *Physical Review E* **88**, 053018 (2013).
 [8] S. M. Davidson, M. B. Andersen, and A. Mani, Chaotic induced-charge electro-osmosis, *Physical review letters* **112**, 128302 (2014).
 [9] A. Pérez, P. Vázquez, J. Wu, and P. Traoré, Electrohydrodynamic linear stability analysis of dielectric liquids subjected to unipolar injection in a rectangular enclosure with rigid sidewalls, *Journal of Fluid Mechanics* **758**, 586 (2014).
 [10] I. Rubinstein and B. Zaltzman, Equilibrium electroconvective instability, *Physical review letters* **114**, 114502 (2015).
 [11] M. Zhang, F. Martinelli, J. Wu, P. J. Schmid, and M. Quadrio, Modal and non-modal stability analysis of electrohydrodynamic flow with and without cross-flow, *Journal of Fluid Mechanics* **770**, 319 (2015).
 [12] P. Traore, J. Wu, C. Louste, P. A. Vazquez, and A. T. Perez, Numerical study of a plane poiseuille channel flow of a dielectric liquid subjected to unipolar injection, *IEEE Transactions on Dielectrics and Electrical Insulation* **22**, 2779 (2015).
 [13] J. Wu and P. Traoré, A finite-volume method for electrothermoconvective phenomena in a plane layer of dielectric liquid, *Numerical Heat Transfer, Part A: Applications* **68**, 471 (2015).
 [14] J. Wu, A. T. Perez, P. Traore, and P. A. Vazquez, Complex flow patterns at the onset of annular electroconvection in a dielectric liquid subjected to an arbitrary unipolar injection, *IEEE Transactions on Dielectrics and Electrical Insulation* **22**, 2637 (2015).
 [15] J. Wu, P. Traoré, A. T. Pérez, and P. A. Vázquez, On two-dimensional finite amplitude electro-convection in a dielectric liquid induced by a strong unipolar injection, *Journal of Electrostatics* **74**, 85 (2015).
 [16] M. Zhang, Weakly nonlinear stability analysis of subcritical electrohydrodynamic flow subject to strong unipolar injection, *Journal of Fluid Mechanics* **792**, 328 (2016).
 [17] K. Luo, J. Wu, H.-L. Yi, and H.-P. Tan, Lattice Boltzmann model for Coulomb-driven flows in dielectric liquids, *Physical Review E* **93**, 023309 (2016).
 [18] K. Luo, J. Wu, H.-L. Yi, and H.-P. Tan, Three-dimensional finite amplitude electroconvection in dielectric liquids, *Physics of Fluids* **30**, 023602 (2018).
 [19] K. Luo, J. Wu, H.-L. Yi, L.-H. Liu, and H.-P. Tan, Hexagonal convection patterns and their evolutionary scenarios in electroconvection induced by a strong unipolar injection, *Physical Review Fluids* **3**, 053702 (2018).
 [20] K. Luo, T.-F. Li, J. Wu, H.-L. Yi, and H.-P. Tan, Mesoscopic simulation of electrohydrodynamic effects on laminar natural convection of a dielectric liquid in a cubic cavity, *Physics of Fluids* **30**, 103601 (2018).
 [21] N. Felici, Phénomènes hydro et aérodynamiques dans la conduction des diélectriques fluides, *Rev. Gén. Electr.* **78**, 717 (1969).
 [22] N. Felici and J. Lacroix, Electroconvection in insulating liquids with special reference to uni- and bi-polar injection: a review of the research work at the CNRS Laboratory for Electrostatics, Grenoble 1969–1976, *Journal of Electrostatics* **5**, 135 (1978).
 [23] J. Schneider and P. Watson, Electrohydrodynamic Stability of Space-Charge-Limited Currents in Dielectric Liquids. I. Theoretical Study, *The Physics of Fluids* **13**, 1948 (1970).

- [24] P. Watson, J. Schneider, and H. Till, Electrohydrodynamic Stability of Space-Charge-Limited Currents in Dielectric Liquids. II. Experimental Study, *The Physics of Fluids* **13**, 1955 (1970).
- [25] P. Atten and R. Moreau, Stabilité électrohydrodynamique des liquides isolants soumis à une injection unipolaire, *J. Mécanique* **11**, 471 (1972).
- [26] J. Lacroix, P. Atten, and E. Hopfinger, Electro-convection in a dielectric liquid layer subjected to unipolar injection, *Journal of Fluid Mechanics* **69**, 539 (1975).
- [27] P. Atten and J. Lacroix, Non-linear hydrodynamic stability of liquids subjected to unipolar injection, *Journal de Mécanique* **18**, 469 (1979).
- [28] P. Atten, Rôle de la diffusion dans le problème de la stabilité hydrodynamique d'un liquide diélectrique soumis à une injection unipolaire forte, *CR Acad. Sci. Paris* **283**, 29 (1976).
- [29] R. Chicón, A. Castellanos, and E. Martín, Numerical modelling of Coulomb-driven convection in insulating liquids, *Journal of Fluid Mechanics* **344**, 43 (1997).
- [30] P. Vazquez, G. Georghiou, and A. Castellanos, Characterization of injection instabilities in electrohydrodynamics by numerical modelling: comparison of particle in cell and flux corrected transport methods for electroconvection between two plates, *Journal of Physics D: Applied Physics* **39**, 2754 (2006).
- [31] S. Chandrasekhar, *Hydrodynamic and hydromagnetic stability* (Courier Corporation, 2013).
- [32] P. G. Drazin and W. H. Reid, *Hydrodynamic stability* (Cambridge university press, 2004).
- [33] E. L. Koschmieder, *Bénard cells and Taylor vortices* (Cambridge University Press, 1993).
- [34] P. Bergé and M. Dubois, Rayleigh-bénard convection, *Contemporary Physics* **25**, 535 (1984).
- [35] M. Krishnan, V. M. Ugaz, and M. A. Burns, PCR in a Rayleigh-Benard convection cell, *Science* **298**, 793 (2002).
- [36] A. V. Getling, *Rayleigh-Bénard Convection: Structures and Dynamics* (World Scientific, 1998), Vol. 11.
- [37] A. Mohamad and R. Viskanta, Laminar flow and heat transfer in Rayleigh-Bénard convection with shear, *Physics of Fluids A: Fluid Dynamics* **4**, 2131 (1992).
- [38] Y. Guan and I. Novosselov, Two Relaxation Time Lattice Boltzmann Method Coupled to Fast Fourier Transform Poisson Solver: Application to Electroconvective Flow, arXiv preprint arXiv:1812.05711 (2018).
- [39] Y. Zhang, L. Liu, Y. Chen, and J. Ouyang, Characteristics of ionic wind in needle-to-ring corona discharge, *Journal of Electrostatics* **74**, 15 (2015).
- [40] Y. Guan, R. S. Vaddi, A. Aliseda, and I. Novosselov, Experimental and Numerical Investigation of Electro-Hydrodynamic Flow in a Point-to-Ring Corona Discharge *Physical Review Fluids* **3**, 14 (2018).
- [41] Y. Guan, R. S. Vaddi, A. Aliseda, and I. Novosselov, Analytical model of electro-hydrodynamic flow in corona discharge, *Physics of plasmas* **25**, 083507 (2018).
- [42] Y. Guan and I. Novosselov, Numerical Analysis of Electroconvection Phenomena in Cross-flow, arXiv preprint arXiv:1812.10899 (2018).